Research Letter DOI: 10.15541/jim20240094

Highly Weak-light Sensitive and Dual-band Switchable Photodetector Based on CuI/Si Unilateral Heterojunction

YANG Jialin[1], WANG Liangjun[1], RUAN Siyuan[1], JIANG Xiulin[2,3], YANG Chang[1]

(1. Key Laboratory of Polar Materials and Devices (MOE), Shanghai Center of Brain-inspired Intelligent Materials and Devices, Department of Electronics, East China Normal University, Shanghai 200241, China; 2. Institute of Intelligent Flexible Mechatronics, Jiangsu University, Zhenjiang 212013, China; 3. Cell R&D Center, JA Solar Holdings Co., Ltd, Yangzhou 225000, China)

Abstract: In recent years, copper iodide (CuI) is an emerging p-type wide bandgap semiconductor with high intrinsic Hall mobility, high optical absorption and large exciton binding energy. However, the spectral response and the photoelectric conversion efficiency are limited for CuI-based heterostructure devices, which is related to the difficulty in fabrication of high-quality CuI thin films on other semiconductors. In this study, a p-CuI/n-Si photodiode has been fabricated through a facile solid-phase iodination method. Although the CuI thin film is polycrystalline with obvious structural defects, the CuI/Si diode shows a high weak-light sensitivity and a high rectification ratio of 7.6×10^4, indicating a good defect tolerance. This is because of the unilateral heterojunction behavior of the formation of the p^+n diode. In this work, the mechanism of photocurrent of the p^+n diode has been studied comprehensively. Different monochromatic lasers with wavelengths of 400, 505, 635 and 780 nm have been selected for testing the photoresponse. Under zero-bias voltage, the device is a unilateral heterojunction, and only visible light can be absorbed at the Si side. On the other hand, when a bias voltage of –3 V is applied, the photodiode is switched to a broader "UV-visible" band response mode. Therefore, the detection wavelength range can be switched between the "Visible" and "UV-visible" bands by adjusting the bias voltage. Moreover, the obtained CuI/Si diode was very sensitive to weak light illumination. A very high detectivity of 10^{13}–10^{14} Jones can be achieved with a power density as low as 0.5 μW/cm^2, which is significantly higher than that of other Cu-based diodes. These findings underscore the high application potential of CuI when integrated with the traditional Si industry.

Key words: copper iodide; heterojunction; photodetector

Transparent conductive materials (TCMs) are crucial in optoelectronics, serving as key components for transparent electrodes in various devices such as photodetectors, photovoltaic cells, and light-emitting diodes (LEDs)[1-3]. However, most TCMs are n-type semiconductors, such as doped In_2O_3, ZnO, and TiO_2[4-6]. In contrast, p-type TCM is still in infancy, and many materials fail to combine preferable optical transparency and conductivity to compete strongly with n-type materials. Transparent electronics depends on the development of a high-performance p-type TCM[7]. The absence of high-performance p-type TCMs hinders not only the realization of transparent electronics through the combination of p-type and n-type TCMs, but also the advancement of highly efficient heterojunctions based on conventional n-Si technologies.

Copper iodide (CuI) is an emerging p-type wide bandgap semiconductor with high intrinsic Hall mobility, high optical absorption and large exciton binding energy[8-11]. High-quality and low-cost γ-CuI thin films have been successfully fabricated using various physical and chemical methods, including sputtering, pulsed laser deposition, thermal evaporation, electrochemical deposition, and iodization, *etc*[12-20]. They have been widely used in various applications such as p-n junctions, transparent electrodes, solar cells, transistors, and thermoelectric devices[21]. Some heterojunction diodes have been investigated, which involve mixing p-CuI with

Received date: 2024-03-01; **Revised date:** 2024-04-09; **Published online:** 2024-04-19
Foundation item: National Natural Science Foundation of China (62074056); Fundamental Research Funds for the Central Universities
Biography: YANG Jialin (1998–), female, Master candidate. E-mail: 51214700087@stu.ecnu.edu.cn
杨佳霖(1998–), 女, 硕士研究生. E-mail: 51214700087@stu.ecnu.edu.cn
Corresponding author: YANG Chang, professor. E-mail: cyang@phy.ecnu.edu.cn
杨 长, 研究员. E-mail: cyang@phy.ecnu.edu.cn

n-type semiconductors such as AgI, a-IGZO, and ZnO[22-24]. For example, Yamada *et al.*[16] demonstrated the photovoltaic effect under ultraviolet (UV) light in a CuI/IGZO heterojunction, establishing the basis for UV photodetectors using CuI. Zhang *et al.*[25] fabricated a heterojunction comprising $CsPbBr_3$ perovskite and CuI to extend the photodetection region into visible light spectrum by utilizing the relatively narrow bandgap of $CsPbBr_3$ perovskite (2.23 eV).

Nevertheless, the reported CuI-based photodetectors, including the CuI/Si diodes[26], mainly detect wavelengths in the UV band. In addition, the difficulty in fabricating high-quality epitaxial thin films of CuI is a drawback to achieve high device performances[8]. Therefore, developing highly sensitive photovoltaic devices using CuI heterojunctions that have a broad and controllable spectral response remains a challenge. Actually, the CuI/Si heterojunctions have practical significance and show potential for combining the benefits of p-type CuI with the established silicon technology. Heterojunction devices can achieve high performance by utilizing the distinctive characteristics of CuI, such as its wide bandgap and high hole mobility, while also upholding the reliability and durability associated with silicon technology.

In this study, a p^+n CuI/Si heterojunction photodiode was produced using a facile and low-cost solid-phase iodination method. It exhibited high sensitivity to weak light and switchable response wavelength range. The findings show the significant potential of CuI when integrated with the traditional semiconductor industry.

1 Experimental

Fig. 1(a) shows the preparation procedure of CuI/Si heterojunctions. The CuI/Si heterojunctions were fabricated by growing the CuI film on Si (100) single crystal substrate through a facile vapor iodination method. The n-type Si substrate has a resistivity of 1–10 Ω·cm and a thickness of 0.5 mm. First, the Si substrate was covered by a mask with hole size of 1.7 mm×1.7 mm. Then, the Cu thin film with thickness of 20 nm was deposited by thermal evaporation. After that, the sample was placed together with iodine particles (I_2, ⩾99.8%, Meryer) into a frosted clear glass vessel, which was heated up to 80 ℃ for the iodization. Similar processes have been previously reported[19]. The Au electrode with a thickness of 100 nm was employed for ohmic contact.

Fig. 1(b) shows the schematic diagram of CuI/Si photodiode structure. Different monochromatic lasers with wavelengths of 400, 505, 635 and 780 nm were selected for testing the photoresponse, and the effective irradiation area was ~2.4 mm^2. The *I-V* characteristic curve of the photodiode was measured using the semiconductor parameter analyzer (Keithley 4200-SCS). The electrical properties of the CuI thin film and the Si substrate were evaluated by Hall effect measurement. The crystalline structure of the samples was analyzed by the X-ray diffraction (XRD, D/MAX-2550, Rigaku Corporation). The photoluminescence (PL) spectra were measured using a Jobin-Yvon LabRAM HR 800 UV micro-Raman instrument with 325 lasers as the excitation source.

2 Results and discussion

2.1 Structural and electrical characteristics of the CuI/Si heterojunction

Fig. 2(a) shows the XRD θ–2θ scans of the obtained CuI thin films with typical diffraction peaks corresponding to (111), (220), and (311) planes of γ-phase CuI[27]. This result indicates that the sample is polycrystalline γ-CuI in the zinc-blende crystal structure. Fig. 2(b, c) show the optical properties of the CuI thin films investigated by optical transmission spectroscopy. The pure CuI sample exhibits an average transmittance of ~75% in the visible region with a near-band-edge emission near 410 nm. Fig. 2(d) shows the scanning electron microscope (SEM) image of the CuI film morphology on the Si surface, which demonstrates a relatively compact growth of the CuI film.

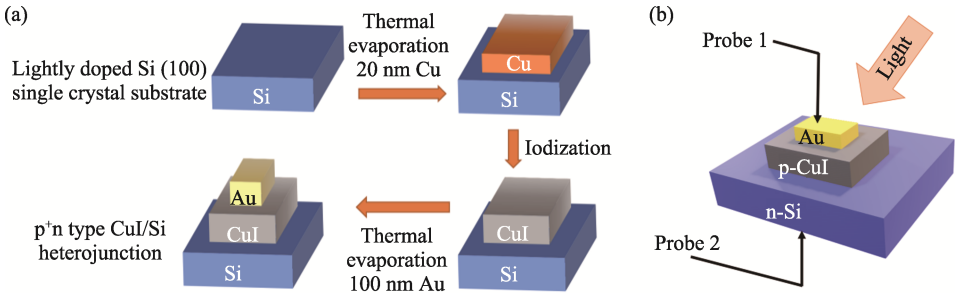

Fig. 1 Fabrication and testing schematic diagram

(a) Schematic structure of the fabricated p^+n type CuI/Si heterojunction diode; (b) Schematic diagram of the photodiode test

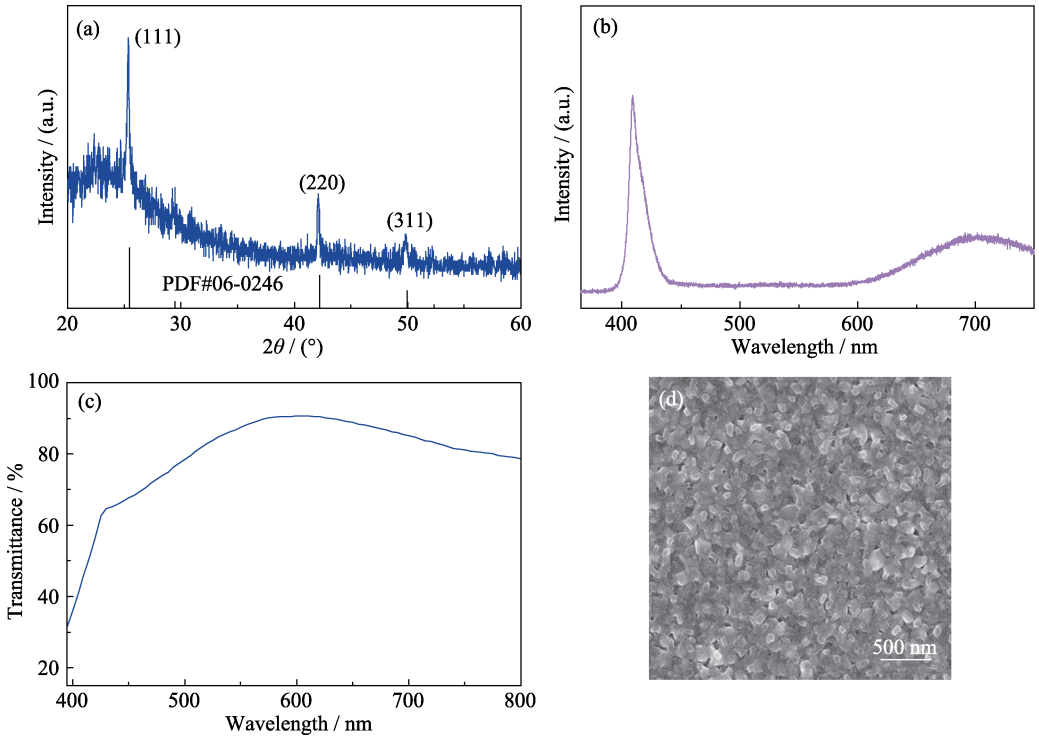

Fig. 2　Structural and electrical characterization of the obtained CuI thin film
(a) XRD pattern; (b) PL spectrum; (c) Optical transmittance; (d) SEM image

Despite of the polycrystalline nature, an ultra-high rectification ratio up to 7.6×10^4 (±3 V) has been observed for the obtained p^+n CuI/Si diode, as shown in Fig. 3. This result is almost the best for CuI-based heterojunctions except for the epitaxial diode in our previous report[8]. The ideal factor of diodes can be deduced from the Shockley equation:

$$j = j_s\left[\exp\left(\frac{qV}{\eta K_B T}\right)-1\right] \quad (1)$$

Where j is the current of diode, j_s is the reverse saturation current density, η is the ideal factor, V is the voltage at the diode, K_B is the Boltzmann constant, T is the absolute temperature of the PN junction, and q is the amount of charge of the electron. In this work, the ideal factor η of ~2.1 indicates the presence of interfacial defects at the heterojunction region, which is similar with most reported heterojunctions made from wide-bandgap semiconductors[28-30]. In addition to the interfacial defects, other factors may also contribute to a large η, such as coupled defect-level recombination[31], deep-level assisted tunneling effect[32], and space-charge-limited conduction[33]. Herein, the effect of interfacial defects should be dominative concerning the polycrystalline nature of the CuI thin film as well as the large lattice mismatch between CuI and Si. As shown in Fig. 2(b), there is a broad emission peak observed at ~700 nm. This is due to the deep-level defects associated with the iodine vacancies[34-35].

Interestingly, it seems that these structural defects have little impact on the device performance, since the dark current shows a value within 10^{-10}–10^{-9} A, which is significantly smaller than those of 10^{-7}–10^{-5} A for other Si-based hetero-diodes in the literature[36-39]. Such a high defect tolerance of the CuI/Si diode might be related to the distribution of the depletion region within the heterojunction. The carrier density of the p-CuI thin film (4.4×10^{19} cm^{-3}) is more than 4 orders of magnitude larger than that of the n-Si substrate (2.0×10^{15} cm^{-3}). That means the CuI/Si here forms a p^+n diode or even a unilateral heterojunction. At zero bias, the Si side depletion depth is estimated to be ~744 nm, whereas the CuI side depletion depth is negligible.

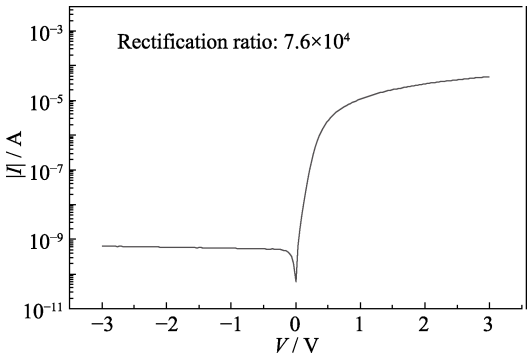

Fig. 3　*I-V* characteristic curve of the CuI/Si heterojunction

2.2 Photodetection properties of the CuI/Si heterojunction

Fig. 4 shows the *I-V* curves of the p^+n CuI/Si photodiode under illumination of laser light with different wavelengths. A small incident light power density in the level of μW/cm^2 is enough to generate a significant photocurrent that is two to three orders of magnitude larger than the dark current, indicating the extremely high weak-light sensitivity of the CuI/Si diode. As a comparison, the detectable light intensity for most reported photodiodes is much higher (in the level of mW/cm^2). The overall photocurrent induced by the 400 nm laser is small, which might be related to the insufficient diffusion length of the minority carriers in the polycrystalline CuI thin film.

At low reverse bias voltage within –0.5 V, the photocurrent rises as the incident laser wavelength increases and gets closer to the Si absorption edge (~1100 nm). Under negative bias voltage, the depletion region of the unilateral heterojunction extends to the CuI side, so that the deep-level defects (Fig. 2(b)) in the CuI thin film partially contribute to the absorption of visible light within 600–800 nm. The 635 nm laser produces a larger saturation photocurrent than the 780 nm laser, since shorter wavelength photons have a greater penetration depth.

The weak-light sensibility was further explored by adjusting the incident light power density. Fig. 5 shows the responsivity R_λ as a function of light power density[40].

$$R_\lambda = I_\lambda / (P_\lambda \times A) \tag{2}$$

Where I_λ is the photocurrent, P_λ is the light power density, and A is the effective contact area of the laser. The responsivity is remarkably high in weak light range (0.5–5 μW/cm^2), and the most sensitive light power density is as low as 0.5 μW/cm^2. Due to equipment restrictions, data for lower light intensities were not gathered. Nevertheless, the existing data already demonstrate the device's high sensitivity to weak light.

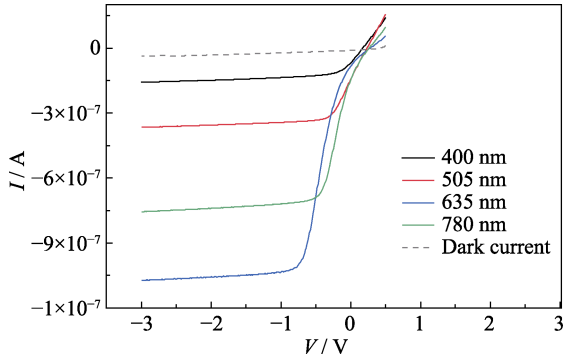

Fig. 4 *I-V* characteristic curves of the CuI/Si photodiode under different laser light wavelengths with a light power density of 50 μW/cm^2

Dark current is plotted in dashed line; Colorful figure is available on website

The spectral response of the CuI/Si photodiode is very different at zero or –3 V bias voltage. Under zero-bias voltage (Fig. 5(a)), the device is a unilateral heterojunction, and only visible light can be absorbed at the Si side. This is a typical "Visible" band response for Si. On the other hand, when a bias voltage of –3 V is applied (Fig. 5(b)), the depletion region extends to the CuI side. In this case, the photodiode is switched to a broader "UV-visible" band response mode, and all lasers at 400–780 nm are detectable. Therefore, the switch of different spectral response ranges can be achieved by adjusting the bias voltage.

The depletion regions of both CuI and Si side are extended at –3 V bias voltage, so the maximum responsivity at –3 V (4.7 A/W for 780 nm) is much higher than that at zero-bias voltage condition (1.15 A/W for 780 nm). However, stronger laser power density results in a lower responsivity, which might be related to the saturation of the photoelectric conversion. Defects in CuI are carrier trapping centers, and produce additional carriers due to the persistent photoconductivity effect. Under strong illumination, the defect trapping centers in CuI reach saturation, so no additional carriers are generated. The corresponding detectivity D^* and external quantum efficiency (EQE) are directly proportional to the responsivity[36] (Table 1).

$$D^* = \frac{R_\lambda}{\sqrt{2eI_{\text{dark}} / S}} \tag{3}$$

$$\text{EQE} = hc \times \frac{R_\lambda}{e\lambda} \tag{4}$$

Where e is the elementary charge, I_{dark} is the dark current, S is the effective contact area of the laser light, h is the Planck constant, c is the speed of light, and λ is the wavelength of the laser.

The maximum D^* is greater than 10^{14} for weak light illumination and ~10^{13} for strong light illumination. These values are record high and more than 100 times greater than other photodetectors made from Cu-based semiconductors, such as CuO photodetectors with $D^* < 10^{11}$[41-42]. Owing to the weak light sensitivity of the obtained CuI/Si diode, the ultra-high EQE of 1109% for 400 nm laser and ~800% for 505–780 nm lasers are achieved at the "UV-visible" response mode (–3 V bias voltage). At the "Visible" response mode (zero bias voltage), the EQE are also high with a maximum of 175% for 635 nm laser. These responsivity and D^* are significantly greater than those of reported Si-based photodiodes (Table 2), demonstrating the high performance of the CuI/Si diode obtained in this work.

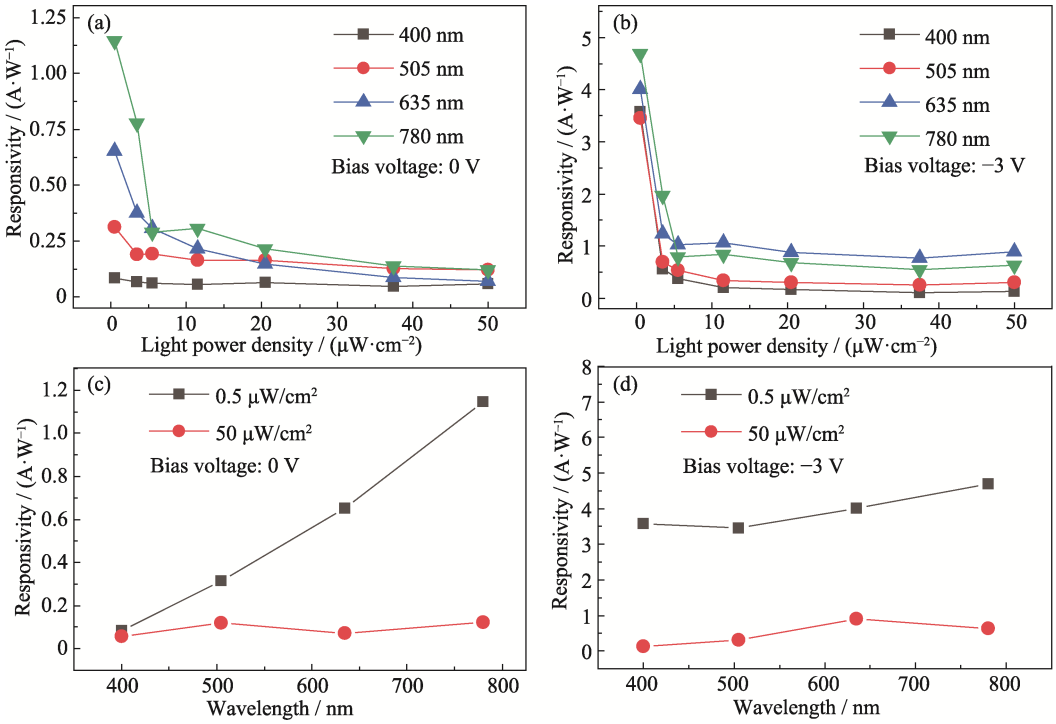

Fig. 5　Responsivity of the CuI/Si photodiode as a function of light power density and responsivity under specific light intensity
(a) 0 V bias applied; (b) –3 V bias applied; (c) 0 V bias applied under specific light intensity; (d) –3 V bias applied under specific light intensity

Table 1　Device parameters of the CuI/Si photodiodes

Wavelength/nm	Bias voltage/V	Responsivity (Weak/strong light)/(A·W^{-1})	D^* (Weak/strong light)/(×10^{13}, Jones)	EQE (Weak/strong light)/%
400	0	0.08/0.06	0.363/0.241	26/17
	–3	3.58/0.15	15.4/0.669	1109/48
505	0	0.31/0.14	1.35/0.618	77/35
	–3	3.46/0.30	14.9/1.31	849/74
635	0	0.65/0.13	2.82/0.561	127/25
	–3	4.00/0.90	17.3/3.88	782/175
780	0	1.15/0.20	4.94/0.844	182/31
	–3	4.70/0.67	20.3/2.92	747/107

Table 2　Summarization of photoelectric properties in Si-based photodiodes

Diode structure	Wavelength/ nm	Power density/ (μW·cm^{-2})	Bias voltage/V	D^*/Jones	Responsivity/ (A·W^{-1})	EQE/%	Ref.
SnSe/Si	405	10	–4	3.4×10^{11}	0.21	–	[36]
	405	300	–4	3.0×10^{11}	0.18	–	
	650	10	0	1.1×10^{11}	0.20	–	
	650	300	0	1.0×10^{11}	0.17	–	
MoS_2/Si	514	3	–2	2.2×10^{11}	1.25	–	[37]
	514	80	–2	8.0×10^{11}	0.90	–	
Graphene-Si	730	10	–2	2.1×10^{8}	0.35	–	[38]
Si/ZnO	550	–	–2	–	0.37	–	[39]
ZnTe-TeO_2/Si	350	–	0	4.0×10^{12}	0.03	–	[43]
	850	–	0	1.4×10^{13}	0.08	–	
CuI/Si	400	0.5	–3	1.54×10^{14}	3.58	1109	This work
	400	50	–3	6.69×10^{12}	0.15	48	
	780	0.5	0	4.94×10^{13}	1.15	182	
	780	50	0	8.44×10^{12}	0.20	31	

3 Conclusions

In summary, a high-performance photodetector based on CuI/Si unilateral heterojunction has been fabricated using a facile solid-phase iodination method. This device exhibits a high rectification ratio of 7.6×10^4 and a low dark current of 10^{-10} A in spite of the polycrystalline structure of CuI. The unilateral diode structure allows for a dual-band switchable behavior. Under zero-bias voltage, the device is a unilateral heterojunction, and only visible light can be absorbed at the Si side. On the other hand, when a bias voltage of –3 V is applied, the photodiode is switched to a broader "UV-visible" band response mode. Therefore, the spectral response can be easily switched between "Visible" and "UV-visible" bands by adjusting the bias voltage. Moreover, the obtained CuI/Si diode is very sensitive to weak light illumination. The responsivity is remarkably high when the light power density is as low as 0.5 μW/cm^2. Ultra-high EQE values of 1109% for 400 nm laser and ~800% for 505–780 nm lasers are achieved at the "UV-visible" response mode. At the "Visible" response mode, the EQE values are also high with a maximum of 175% for 635 nm laser. These findings demonstrate the significant potential for applying CuI in combination with the traditional semiconductor industry.

References:

[1] YU X, MARKS T, FACCHETTI A. Metal oxides for optoelectronic applications. *Nature Materials*, 2016, **15:** 383.

[2] WOODS-ROBINSON R, HAN Y B, ZHANG H Y, *et al*. Wide band gap chalcogenide semiconductors. *Chemical Reviews*, 2020, **120(9):** 4007.

[3] ZHANG C, NICOLOSI V. Graphene and MXene-based transparent conductive electrodes and supercapacitors. *Energy Storage Materials*, 2019, **16:** 102.

[4] FANG H, ZHAO Z, WU W, *et al*. Progress in flexible electrochromic devices. *Journal of Inorganic Materials*, 2021, **36(2):** 140.

[5] LIU H, LI H, TAO J, *et al*. Single crystalline transparent conducting F, Al, and Ga Co-doped ZnO thin films with high photoelectrical performance. *ACS Applied Materials & Interfaces*, 2023, **15(18):** 22195.

[6] YUTAKA F, TARO H, YUKIO Y, *et al*. A transparent metal: Nb-doped anatase TiO_2. *Applied Physics Letters*, 2005, **86(25):** 252101.

[7] WILLIS J, SCANLON D. Latest directions in p-type transparent conductor design. *Journal of Materials Chemistry C*, 2021, **9:** 11995.

[8] YANG C, KNEISS M, SCHEIN F L, *et al*. Room-temperature domain-epitaxy of copper iodide thin films for transparent CuI/ZnO heterojunctions with high rectification ratios larger than 109. *Scientific Reports*, 2016, **6:** 21937.

[9] LI Z, HE J, LV X, *et al*. Optoelectronic properties and ultrafast carrier dynamics of copper iodide thin films. *Nature Communications*, 2022, **13:** 6346.

[10] YANG C, MAX K, MICHAEL L, *et al*. Room-temperature synthesized copper iodide thin film as degenerate p-type transparent conductor with a boosted figure of merit. *Applied Physical Sciences*, 2016, **113(46):** 12929.

[11] MARIUS G, FRIEDRICH S, MICHAEL L, *et al*. Cuprous iodide-a p-type transparent semiconductor: history and novel applications. *Physica Status Solidi A*, 2013, **210(9):** 1671.

[12] TANAKA T, KEISHI K, MASATAKA H. Transparent, conductive CuI films prepared by rf-dc coupled magnetron sputtering. *Thin Solid Films*, 1996, **281:** 179.

[13] KIM D, NAKAYAM M, KOJIM O, *et al*. Thermal-strain-induced splitting of heavy and light-hole exciton energies in CuI thin films grown by vacuum evaporation. *Physical Review B*, 1999, **60(19):** 13879.

[14] ZI M, LI J, ZHANG Z, *et al*. Effect of deposition temperature on transparent conductive properties of γ-CuI film prepared by vacuum thermal evaporation. *Phys. Status Solidi*, 2015, **212:** 1466.

[15] KANG H, LIU R, CHEN K, *et al*. Electrodeposition and optical properties of highly oriented γ-CuI thin films. *Electrochim Acta*, 2010, **55(27):** 8121.

[16] YAMADA N, KONDO Y, INO R. Low-temperature fabrication and performance of polycrystalline CuI films as transparent p-type semiconductors. *Physica Status Solidi*, 2019, **216(5):** 1700782.

[17] STORM P, BAR M, BENNDORF G, *et al*. High mobility, highly transparent, smooth, p-type CuI thin films grown by pulsed laser deposition. *APL Materials*, 2020, **8(9):** 091115.

[18] YANG C, ROSE E, YU W, *et al*. Controllable growth of copper iodide for high-mobility thin films and self-assembled micro-crystals. *ACS Applied Electronic Materials*, 2020, **2(11):** 3627.

[19] GENG F, WU Y, SPLITH D, *et al*. Amorphous transparent Cu(S,I) thin films with very high hole conductivity. *Journal of Physical Chemistry Letters*, 2023, **14(26):** 6163.

[20] GENG F, WANG L, STRALKA T, *et al*. (111)-oriented growth and acceptor doping of transparent conductive CuI:S thin films by spin coating and radio frequency-sputtering. *Advanced Engineering Materials*, 2023, **25(11):** 2201666.

[21] YANG C, SOUCHAY D, KNEISS M, *et al*. Transparent flexible thermoelectric material based on non-toxic earth-abundant p-type copper iodide thin film. *Nature Communications*, 2017, **8:** 16076.

[22] CHA J, JUNG D. Air-stable transparent silver iodide-copper iodide heterojunction diode. *ACS Applied Materials Interfaces*, 2017, **9(50):** 43807.

[23] NAOOMI Y, YUUMI K, XIANG C, *et al*. Visible-blind wide-dynamic-range fast-response self-powered ultraviolet photodetector based on CuI/In-Ga-Zn-O heterojunction. *Applied Materials Today*, 2019, **15:** 153.

[24] AKSHAI S, NANDAKUMAR A, RAMESH R, *et al*. Self-powered UV photodetectors based on heterojunctions composed of ZnO nanorods coated with thin films of ZnS and CuI. *ACS Applied Nano Materials*, 2023, **6(10):** 8529.

[25] ZHANG Y, LI S, YANG W, *et al*. Millimeter-sized single-crystal $CsPbrB_3$/CuI heterojunction for high-performance self-powered photodetector. *Journal of Physical Chemistry Letters*, 2019, **10(10):** 2400.

[26] WANG Y, CHUANG C. Solution processed CuI/n-Si junction device annealed with and without iodine steam for ultraviolet photodetector applications. *Journal of Materials Science*, 2018, **29(21):** 18622.

[27] LI W, SHI W. Growth habit and habit variation of γ-CuI crystallites under hydrothermal conditions. *Crystal Research & Technology*, 2002, **37(10):** 1041.

[28] ALIVOV Y, ÖZGÜR Ü, DOĞAN S, *et al*. Photoresponse of n-ZnO/p-SiC heterojunction diodes grown by plasma-assisted molecular-beam epitaxy. *Applied Physics Letters*, 2005, **86(24):** 241108.

[29] LEE M, SEO S, KIM D, *et al*. A low-temperature grown oxide

diode as a new switch element for high-density, nonvolatile memories. *Advanced Materials*, 2007, **19(1):** 73.
[30] BRÖTZMANN M, VETTER U, HOFSÄSS H. BN/ZnO heterojunction diodes with apparently giant ideality factors. *Journal of Applied Physics*, 2009, **106(6):** 063704.
[31] SCHENK A, KRUMBEIN U. Coupled defect level recombination: theory and application to anomalous diode characteristics. *Journal of Applied Physics*, 1995, **78(5):** 3185.
[32] YASUHISA O, YOSHIAKI M, SHINGO S, *et al*. Revisiting the role of trap-assisted-tunneling process on current-voltage characteristics in tunnel field-effect transistors. *Journal of Applied Physics*, 2018, **123(16):** 161549.
[33] TALIN A, ALEC, LEONARD F, SWART B, *et al*. Unusually strong space-charge-limited current in thin wires. *Physical Review Letters*, 2008, **101:** 076802.
[34] YU W, BENNDORF G, JIANG Y, *et al*. Control of optical absorption and emission of sputtered copper iodide thin films. *Physica Status Solidi (RRL)-Rapid Research Letters*, 2020, **15(1):** 2000431.
[35] YANG Y, SHAO Y, LI B, *et al*. Enhanced band-edge luminescence of CuI thin film by Cl-doping. *Journal of Inorganic Materials*, 2023, **38(6):** 687.
[36] LUO F, ZHOU H, LIU Y, *et al*. High-performance self-driven SnSe/Si heterojunction photovoltaic photodetector. *Chemosensors*, 2023, **11:** 406.
[37] MUKHERJEE S, MAITI R, KATIYAR A, *et al*. Novel colloidal MoS_2 quantum dot heterojunctions on silicon platforms for multifunctional optoelectronic devices. *Scientific Reports*, 2016, **6:** 29016.
[38] AN X, LIU F, JUNG Y, *et al*. Tunable graphenesilicon heterojunctions for ultrasensitive photodetection. *Nano Letters*, 2013, **13(3):** 909.
[39] LIM S, UM D, HA M, *et al*. Broadband omnidirectional light detection in flexible and hierarchical ZnO/Si heterojunction photodiodes. *Nano Research*, 2017, **10:** 22.
[40] SAHATIYA P, REDDY C, BADHULIKA S. Discretely distributed 1D V_2O_5 nanowires over 2D MoS_2 nanoflakes for an enhanced broadband flexible photodetector covering the ultraviolet to near infrared region. *Journal of Materials Chemistry C*, 2017, **5(48):** 12728.
[41] YIN W, YANG J, ZHAO K, *et al*. High responsivity and external quantum efficiency photodetectors based on solution-processed Ni-doped CuO films. *ACS Applied Materials & Interfaces*, 2020, **12(10):** 11797.
[42] HONG Q, CAO Y, HU J, *et al*. Self-powered ultrafast broadband photodetector based on p-n heterojunctions of CuO/Si nanowire array. *ACS Applied Materials & Interfaces*, 2014, **6(23):** 20887.
[43] SONG Z, LIU Y, WANG Q, *et al*. Self-powered photodetectors based on a ZnTe-TeO_2 composite/Si heterojunction with ultrabroadband and high responsivity. *Journal of Materials Science*, 2018, **53:** 7562.

基于 CuI/Si 单边异质结的微光高灵敏双波段可切换光电探测器

杨佳霖[1], 王亮君[1], 阮丝园[1], 蒋秀林[2,3], 杨 长[1]

(1. 华东师范大学 电子系, 极化材料与器件教育部重点实验室, 上海类脑智能材料与器件研究中心, 上海 200241;
2. 江苏大学 智能柔性机械电子研究院, 镇江 212013; 3. 晶澳太阳能有限公司 电池研发中心, 扬州 225000)

摘 要: 近年来, 碘化铜(CuI)因其较高的本征霍尔迁移率、高光吸收和较大的激子结合能而成为一种新兴的 p 型宽带隙半导体。然而, 在传统半导体材料表面制备高质量 CuI 薄膜非常困难, 已有 CuI 基异质结器件的光谱响应和光电转换效率较低。本研究采用一种简易的金属碘化法制备了一种 p-CuI/n-Si 结构的光电二极管。虽然获得的 CuI 是带有明显结构缺陷的多晶薄膜, 但 CuI/Si 二极管具有很高的弱光灵敏度。其高达 7.6×10^4 的整流比表明该光电二极管具有良好的缺陷容忍度, 这与 p^+n 型二极管的单边异质结这一特殊结构有关。本研究对该 p^+n 型二极管的光电响应进行了较为系统的研究, 选择波长分别为 400、505、635 和 780 nm 的不同单色激光器进行光响应测试。在零偏置电压条件下, 该器件为单边异质结, 耗尽层仅在硅一侧, 因此只有可见光被吸收。当施加–3 V 的偏置电压时, 光电二极管被切换到“紫外-可见”双波段响应的工作模式。因此, 通过调整偏置电压可以使检测波长在“可见”波段和“紫外-可见”波段之间切换。此外, 本研究所得到的 CuI/Si 二极管对弱光照非常敏感。在入射光功率密度低至 0.5 μW/cm^2 时, 其具有高达 10^{13}~10^{14} Jones 的探测率, 明显优于其他铜基光电二极管。相关研究结果证实了 CuI 在与传统硅工业集成时的高应用潜力。

关 键 词: 碘化铜; 异质结; 光电探测器

中图分类号: TQ174 **文献标志码:** A **文章编号:** 1000-324X(2024)09-1063-07